Journal of Alloys and Compounds, 207/208 (1994) 1–13
JALCOM 3005

Exploring the black oxide of praseodymium

LeRoy Eyring
Department of Chemistry and Biochemistry and The Center for Solid State Science, Arizona State University, Tempe, AZ 85287-1604 (USA)

1. Introduction

I want to thank the person who considered me a worthy candidate for the Spedding Award, those who supported the suggestion as not entirely ridiculous, and the committee for their favorable action. This is a great honor that I fully appreciate. Well, the others were so young and their time will come.

This conference has become a remarkable agent for facilitating rare earth science in its broadest sense. The history of the Spedding award certifies the breadth of interests of the conference. The multidisciplinary foundation was laid at the first conference organized in 1960 by Eugene V. Kleber at Lake Arrowhead, California. I tell you with some pride that one of my students, Karl Vorres, organized the third conference in 1963 at Clearwater, Florida. (He actually planned it for Bermuda but our patrons in the nations capitol squelched his ambitious plan.) We held the third conference in 1964 at Camelback Inn in Phoenix. The tenth, hosted by our colleague Therald Moeller, was also held in 1973 in the Phoenix area, this time at the Carefree Inn. The eleventh was held in 1974 in Traverse City, Michigan hosted by my two colleagues Harry Eick and John Haschke.

It was at Lake Arrowhead that I was persuaded to assume the editorship of what was to be called *Progress in the Science and Technology of the Rare Earths*, published by Pergamon, when R.C. Vickery, who originated the idea, decided not to continue. The series fizzled after three volumes. It needed Karl Gschneidner, who unfortunately was then just a boy.

Several of the planners and organizers of the first conference had also organized the forerunner of what became Rare Earth Research, Inc., recently acquired by Rhône-Poulenc, the financial underwriters of the Spedding Award to whom I especially wish to express my gratitude. Worthy endeavors require generous patrons.

My first encounter with Frank Spedding was indirect. A proposal of a new line of research was required at Berkeley for the qualifying examination. I came up for mine in 1947, the year Spedding and his associates published their war-time work on the large-scale separation of the rare earths by column exchange. This was a fantastic breakthrough for all of us needing pure specimens for research. The discovery of element 61 had also just been announced. I proposed a research program based on the promised availability of these fascinating elements about which there was relatively so little known.

Quite fortuitously my first position was at the State University of Iowa (not to be confused with Iowa State University, Spedding's stronghold). It was the custom in those days that faculty members from the two Iowa schools would alternate locations for social and scientific get togethers. The last one was held in Iowa City, my second year there. On that occasion I screwed up the courage to tell Spedding, of whom I was in great awe, about our strange experiences with the higher oxides of praseodymium. I considered his interest and encouragement on that occasion a seal of approval on our project. He mentioned the unusual double hexagonal structures his people were finding in the metals. I saw him from a distance when I visited Ames occasionally over the next 30 years before his death.

There is a story about Herbert M. McCoy giving a pound of europium and three pounds of samarium, obtained by fractional crystallization, to Spedding when he was just getting started in rare earth research. In a similar spirit, Spedding provided us with praseodymium oxide 99.9% pure for US$25 a gram when we were paying US$1000 a gram for oxides only 98% pure. Much earlier, I remember buying gadolinium oxide that was 55% lanthanum. Had Spedding done nothing else than provide rare earths of high purity for general research, he should have deserved our undying gratitude.

As an alternative to being brilliant, one way to win the Spedding Award is to spend a lifetime focusing

SSDI 0925-8388(93)03005-4

your own interest and that of your students on rare earth science. That is true in my case. I was captivated in graduate school with praseodymium oxide which we were using as a stand-in for americium. My research adviser, Burris Cunningham, was just opening up the study of the chemistry of this recently synthesized element and about a milligram was made available to us. Burris had both Larry Asprey and myself working on the thermodynamics of americium oxide, Larry making oxide-oxygen equilibrium measurements and me doing solution micro-calorimetry to obtain the oxidation potential of the +3–+4 couple all on one milligram of oxide. As I said, we used praseodymium as a stand-in for americium to develop our techniques. Trying to prepare the dioxide for calorimetric studies and observing Asprey's incredible tensimetric results hooked me on the higher rare earth oxides for life.

'Flower in the crannied wall,
I pluck you out of the crannies,
I hold you here, root and all, in my hand,
Little flower – but if I could understand
What you are, root and all, and all in all,
I should know what God and man is.'
Alfred Lord Tennyson

In this brief moment together I wish to present a thin slice through the heart of our experience with the dark oxides of praseodymium and terbium. In doing so, the capable work of many of my able collaborators must go unmentioned. This is a pity.

The black oxide of praseodymium has quite a romantic history. Auer von Welsbach, the discoverer of neodidymium and praseodidymium called the black oxide of praseodidymium 'Pr_5O_9' in 1885 [1]. (That is what Auer von Welsbach called them. Their names were later shortened to their present spelling, perhaps partly due to earlier objections by Wöhler that didymium sounded like baby talk.) Prandtl mentioned in 1925 that the composition Pr_5O_9 was still assigned the black oxide in some quarters [2]. Prandtl himself favored thinking of these oxides as praseodymium praseodymates, mixtures of Pr_2O_3 and Pr_2O_5 [3].

There was a great effort in those days to place the rare earths among the elements in the periodic table of the elements. It was plausible that Pr would be pentavalent with V, Nb, and Ta following Ce being tetravalent with Ti, Zr, and Hf, and trivalent La following Sc and Y in the periodic table. Prandtl's work seemed to support pentavalence in praseodymium. Before the end of the 1920s, Pagel and Brinton [4] had established Pr_6O_{11} as the oxide obtained when specimens were cooled from high temperatures in air. In the 1930s, Marsh established the highest oxide as PrO_2 [5]. Marsh was supported in this determination by McCullough who made X-ray diffraction measurements on the pure and mixed oxides and published his results around 1950 [6].

It was McCullough who had established an X-ray lab at Berkeley when, as graduate students, Larry Asprey and I were getting excited about praseodymium oxides. Here we are in 1993, more than a hundred years after Auer von Welsbach first saw the black oxide of a relatively pure praseodymium, and many aspects of the system are still not understood. It is my desire tonight to relate some highlights of our own adventures with this mysterious black oxide.

What I am about to say involves only three elements and, for the most part, only two at any one time. These are praseodymium, terbium and oxygen. Furthermore, we consider only a few variables to fix the conditions of our measurements, usually temperature and oxygen pressure and an electron beam. Even so, the story is fairly complicated and has involved many people over more than a century. Imagine the gargantuan task of knowing what the flower 'root and all, and all in all' is! There seems no limit to the mysteries to be solved.

2. Thermodynamics

The dependence of praseodymium oxide composition on oxygen pressure at constant temperature is shown in Fig. 1 [7]. This is a spectacular exhibition of non-stoichiometry, intermediate phases with narrow composition ranges, and hysteresis. Some of these phenomena were known, for example, in some hydrides and in the heavy transition metal oxides being studied by Magnéli and Wadsley, but were not well understood in those days. When our paper was submitted for publication, one of the reviewers declared it a 'bold and unconvincing narrative', he/she was a better student of Gilbert and Sullivan than of praseodymium oxides.

The dependence of praseodymium oxide composition on temperature at constant oxygen pressure is shown by the selections of isobars, presented in Fig. 2. The phase diagram of the system derived from these and other isobars is shown in Fig. 3 [8,9]. The isothermal and isobaric techniques complement each other by emphasizing different aspects of the system. For example, the homologous series with generic formula Pr_nO_{2n-2} and the non-stoichiometric phases (the σ-phase, $1.50 < x < 1.71$, and the α-phase, $1.72 < x < 2.00$) are much more clearly delineated in the isobaric work.

3. Structures

3.1. X-Ray powder diffraction

Diffraction maxima from X-ray powder patterns established the structures of the higher intermediate oxides

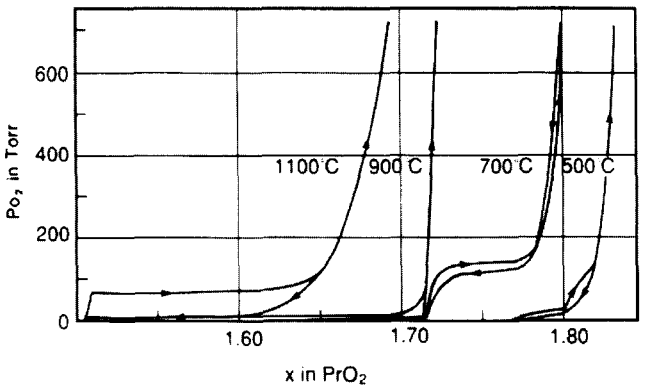

Fig. 1. The dependence of praseodymium oxide composition on oxygen pressure at constant temperature. After Ferguson *et al.* [7].

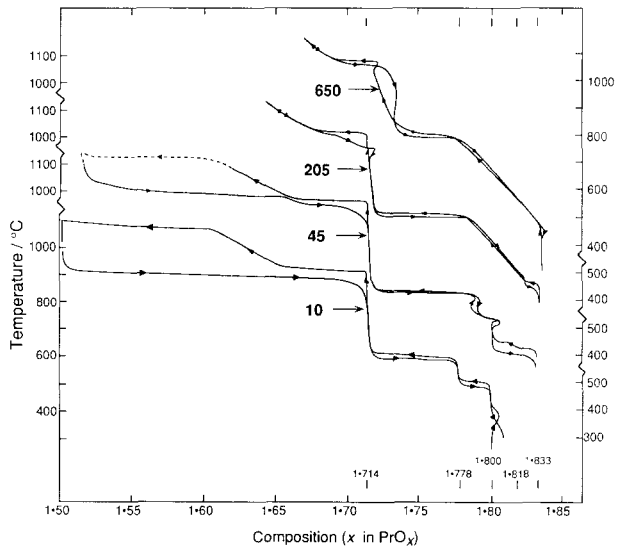

Fig. 2. The dependence of praseodymium oxide composition on temperature at constant oxygen pressure. After Hyde *et al.* [8] and Kordis and Eyring [25].

to be superstructures of fluorite [10]. The careful X-ray studies revealed the splitting of the fluorite substructure lines as well as the existence of the much weaker superstructure lines. However, it was still not possible to determine the unit cells of the homologous series.

3.2. *The unit cells revealed by HREM*

The electron diffraction patterns of several members of the homologous series are shown in Fig. 4 [11]. Projections of the unit cells derived from the electron diffraction patterns are shown, along the common *a*-axis, $[2\,1\,-1]_F$, in Fig. 5.

3.3. *HREM studies of structure*

High-resolution images of the higher oxides were not inconsistent with the predicted structures of the iota and zeta phases ($n=7$, 9) [12,13]. The model for

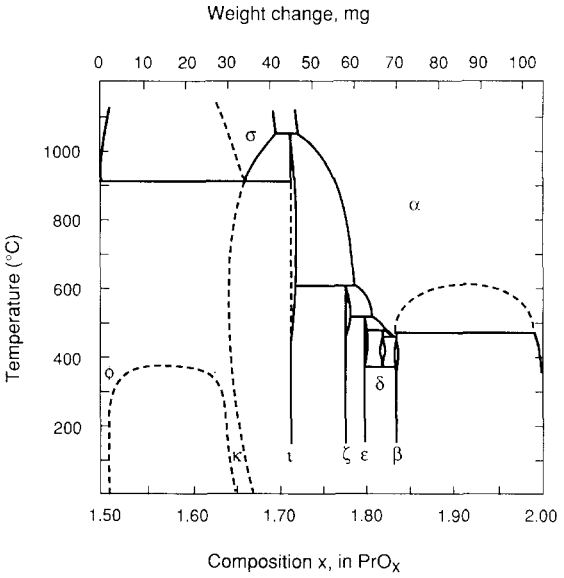

Fig. 3. The phase diagram for praseodymium oxide. After Hyde *et al.* [8] and Turcotte *et al.* [9].

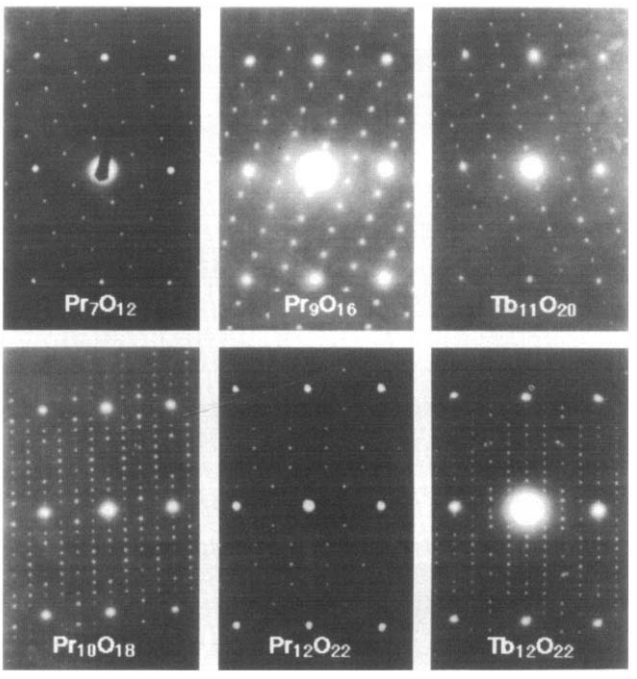

Fig. 4. The electron diffraction patterns of members of the homologous series of higher oxides of praseodymium and terbium in the $[2\,1\,-1]_F$ zone. After Kunzmann and Eyring [11].

simulation [14] assumed double oxygen vacancies along [1 1 1] as were established [15] for Pr_7O_{12}. With this in mind, this di-vacancy defect cluster was assigned to all members of the homologous series [16]. The HREM images show the right number of vacant oxygen sites in the unit cells but the morphology of the specimen and the microscope settings are not well enough known to allow one to match the calculated and observed images convincingly. An HREM image of $Pr_{24}O_{44}$ il-

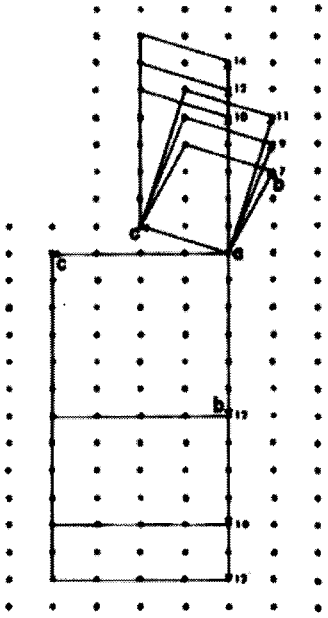

Fig. 5. The projections of the unit cells of members of the homologous series along $[2\,1\,-1]_F$. Derived from the electron diffraction patterns. After Kunzmann and Eyring [11].

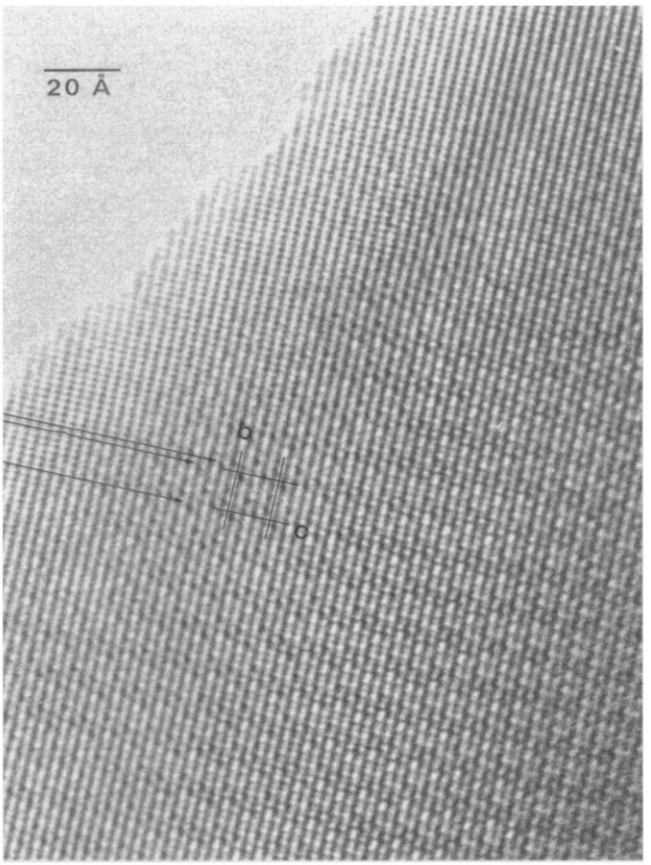

Fig. 6. An HREM image of $Pr_{24}O_{44}$. The unit cell is outlined. After Schweda *et al.* [16].

lustrates the problem (Fig. 6) since it suggested a model later found to be incorrect [16].

3.4. Neutron diffraction and Rietveld analysis

Neutron powder diffraction data have been collected on six members of the Pr and Tb homologous series and their structures determined using the Rietveld analysis method, GSAS [17]. The models established for refinement of the structures required defect clusters of two types. These models are represented in Fig. 7. One is the di-vacancy originally proposed and later found for $n=7$, 9 and 10 but the other has a single vacant oxygen site at its core and is required to model the structures of the more oxidized members. The metal atoms around a vacant oxygen site move outwards about 0.018 nm, while the nearest-neighbor oxygens move inwards about 0.03 nm. The vacancy cluster may be written $V_0Pr_4O_6$. The projections of the known structures down the $[2\,1\,-1]_F$ direction are presented in Fig. 8.

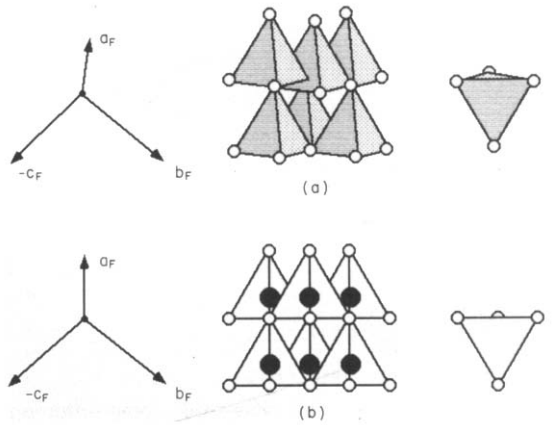

Fig. 7. Clusters at vacant oxygen sites in the fluorite-related rare earth intermediate phases. After Zhang *et al.* [17].

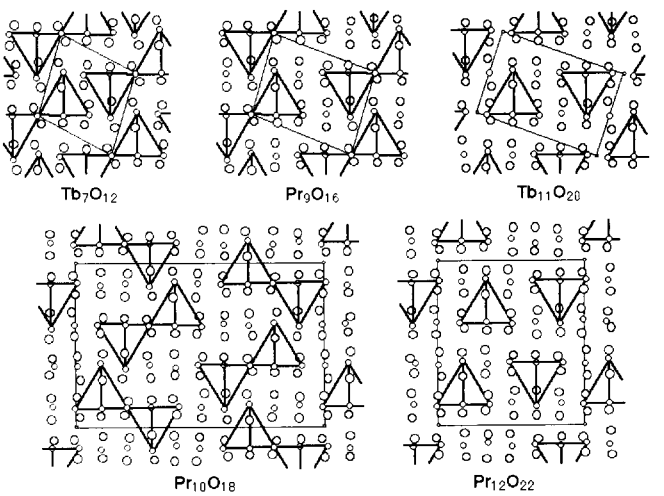

Fig. 8. Projections of the known structures of the higher oxides of the rare earths along $[2\,1\,-1]_F$. After Zhang *et al.* [17].

Four basic architectural rules have been abstracted from the known structures. A vacancy arrangement is unfavorable if:

(a) the vacancy–vacancy distance is shorter than $1/2\langle 1\,1\,1\rangle_F$ (*i.e.* $1/2\langle 1\,0\,0\rangle_F$ or $1/2\langle 1\,1\,0\rangle_F$
(b) the vacancy–vacancy distance is $1/2\langle 1\,1\,1\rangle_F$ but without a metal atom in between
(c) more than two vacancies form aggregates where the vacancy–vacancy distances are of the $1/2\langle 1\,1\,1\rangle_F$ type
(d) the vacancy–vacancy distance is of the $\langle 1\,1\,0\rangle_F$ type so that the oxygen atoms from different coordination defects ($V_0R_4O_6$) overlap.

4. An HREM study of disproportionation of $Tb_{11}O_{20}$ induced by dilute acid

4.1. Equipment and specimen used for the in situ studies

The electron microscopy was accomplished on a JEOL 4000 EX microscope with a point-to-point resolution of 1.6 Å. The video recording was made utilizing a YAG detector and a low-light video camera. The video recorder was a Panasonic 3/4 inch industrial standard. The video processing and editing was accomplished by means of a Macintosh-Sony-Radius system utilizing a suite of programs that included Digital Micrograph, Photoshop, and Debabelizer.

4.2. The mechanism of the disproportionation (leaching) reaction

A TbO_2 specimen was obtained from the leaching of $Tb_{11}O_{20}$ with dilute acid by a disproportionation reaction. The leaching mechanism, clarified by HREM [18], is represented by the equations

$$28e^-_{surf} + 4(Tb_{11}O_{20})_{surf} \longrightarrow 22(Tb_2O_3)_{surf} + 14O_{surf}$$

$$x(Tb_2O_{3surf} + 6H^+_{aq} \longrightarrow 2Tb^{3+}_{aq} + 3H_2Oliq$$

$$y(Tb_2O_{3surf} + 3H_2O_{aq} \longrightarrow 2Tb(OH)_{3surf})$$

$$x + y = 22$$

$$14O_{surf} \rightarrow 14O_{int}$$

$$28e^-_{int} \longrightarrow 28e^-_{surf}$$

$$7(Tb_{11}O_{20})_{int} + 14O_{int} \rightarrow 77(TbO_2)_{int} + 28e^-_{int}$$

where surf = surface, int = interior.

All the Pr was found to go into solution as Pr^{3+} ions at the surface reaction site. The reduction itself is a solid-state reaction. Electrons diffuse to the surface reduction zone from the interior where oxidation has occurred while oxygens diffuse away from the surface to the oxidation zone until the leaching of Pr^{3+} is complete throughout the crystal. The high magnification image and the high resolution image shown in Figs. 9(a, b) are the basis of this proposed mechanism. The

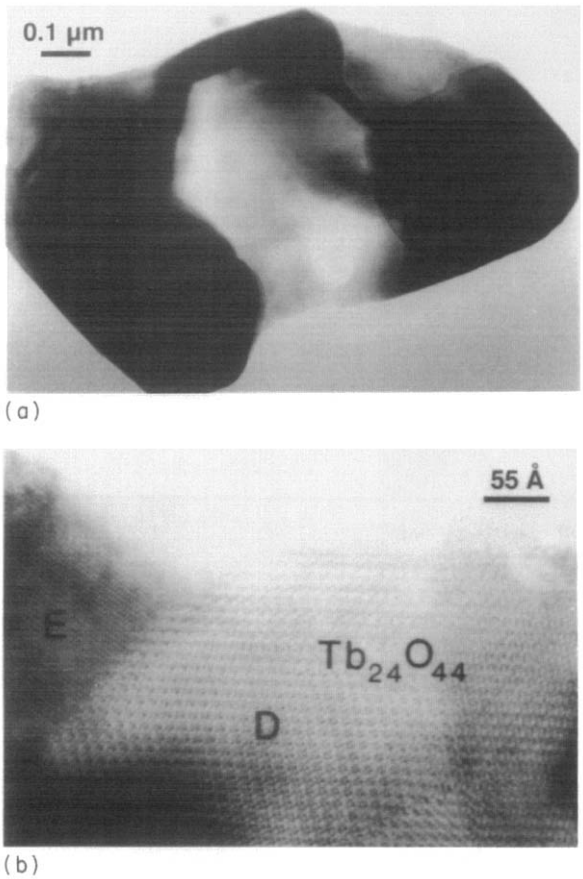

Fig. 9. (a) A high-magnification image of a leached $Tb_{11}O_{20}$ crystal. After Kang and Eyring [18]. (b) A high resolution image of a disproportionation center at the surface of a leached $Tb_{11}O_{20}$ crystal. After Kang and Eyring [18].

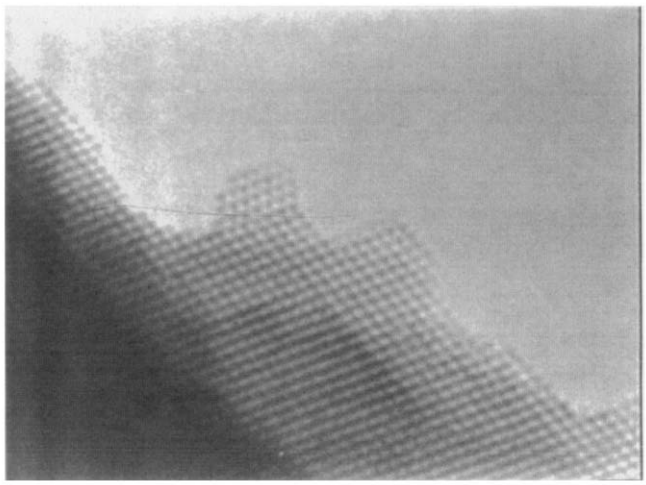

Fig. 10. A twinned promontory left on the crystal surface after leaching a $Tb_{11}O_{20}$ crystal. After Kang *et al.* [19] and Kang and Eyring [20].

reaction sites have been observed in the microscope to be surface defects such as emerging dislocations.

5. Dynamic atomic-level changes observed in situ in HREM in a 1200 atom TbO_2 promontory

The leaching reaction left a promontory on the surface estimated to consist of about 1200 atoms [18,19]. Two-frame images (Fig. 10) of the HREM video recording show this promontory to be in a twinned relationship with the main body of the crystal. The twin plane separating the promontory from the substrate is $\{1\ 1\ 1\}_F$.

5.1. The in situ dynamic changes

The surface profile of the promontory was observed to fluctuate due to rapid motion of surface atoms. These changes are demonstrated in Fig. 11 (sequential two-frame averages show the rapid reconstruction as atoms dance over the surface). The sequence demonstrates the rapid surface modification that continued for 10 min without altering the twin plane.

The video record shows the disordering ('melting') of the entire promontory that occurred suddenly prior to its recrystallization and accretion. Figure 12 shows two-frame averages taken during the instant of disorder preceding recrystallization which then began immediately at the $\{1\ 1\ 1\}_F$ twin plane interface. Within a few seconds, accretion was complete. Figure 13 registers

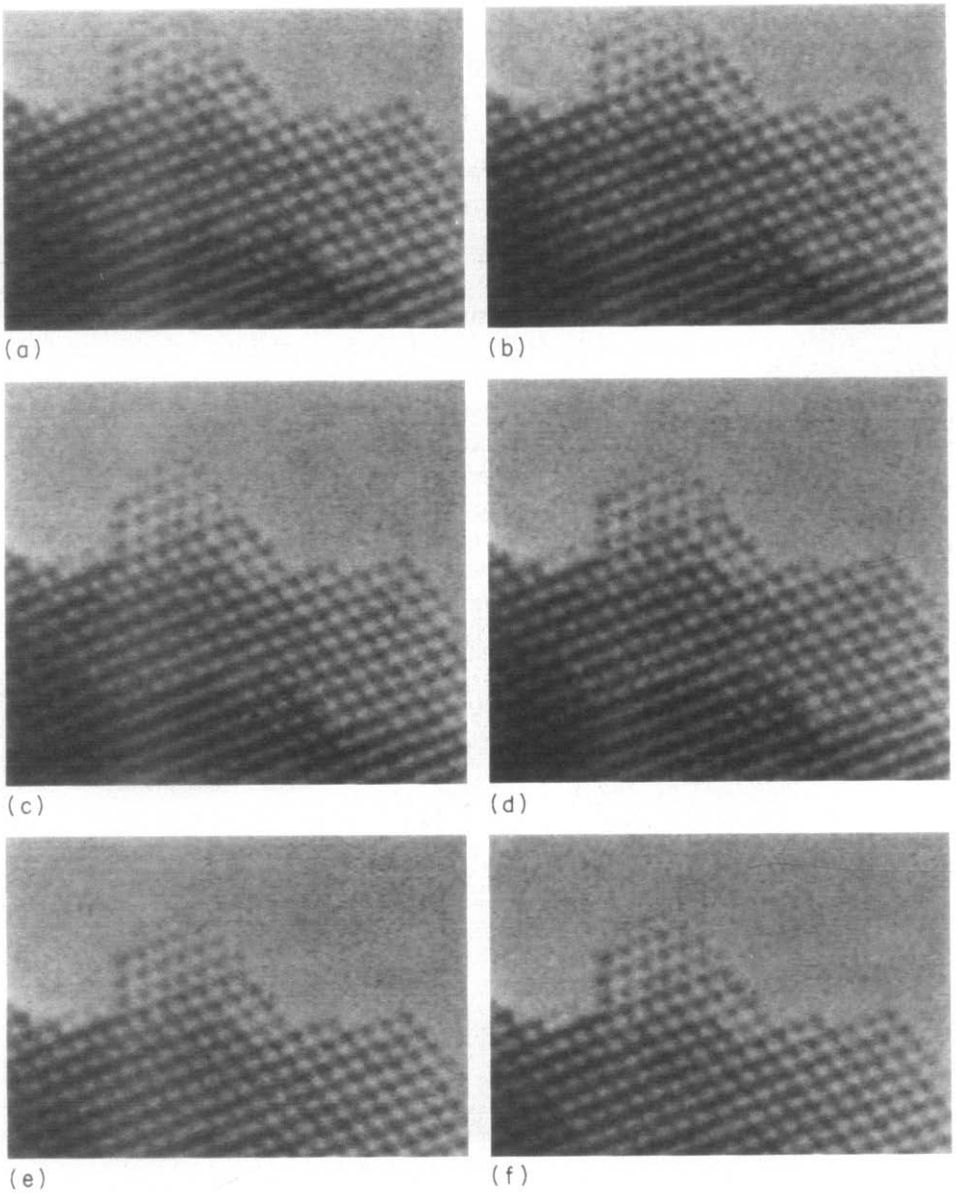

Fig. 11. (a)–(f) Successive two-frame average images of surface profile changes of the promontory in TbO_x (1/30th second intervals).

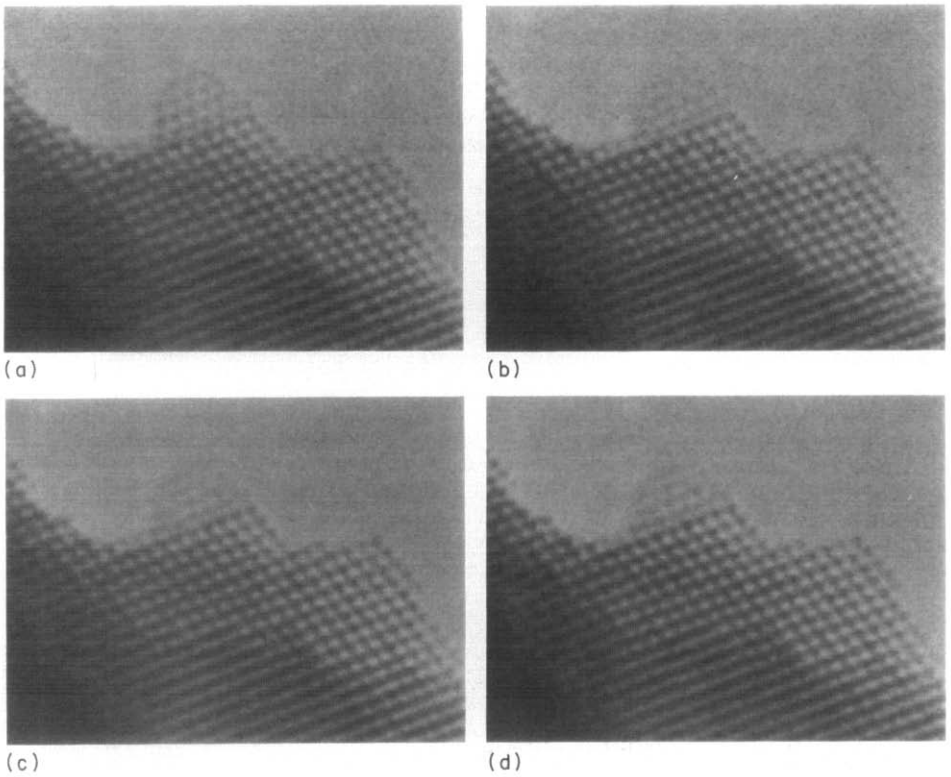

Fig. 12. Successive two-frame average images of the pre-transition disordering of the promontory (1/30th second intervals).

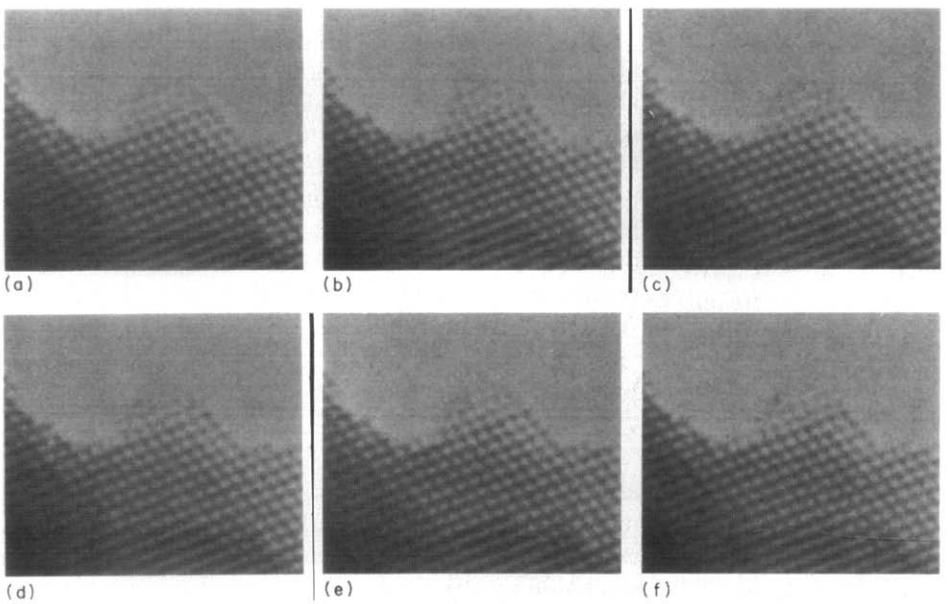

Fig. 13. (a)–(f) A sequence of two-frame average images during recrystallization of the promontory (1/30 second intervals).

two-frame averages during the advance of the boundary into the disordered material of the promontory. Figure 14 shows four-frame averages of the initial and final condition of the promontory. The failure of the twinned promontory to reorient during long irradiation prior to 'melting' must be due to the absence of a mobile ledge of some kind.

6. In situ observation of the decomposition of $Pr(OH)_3$ to the oxide

Residues of $Pr(OH)_3$ formed during the disproportionation reaction are evident at the surface in all the micrographs taken of the solid product [19]. An enclave of hydroxide is shown as a four-frame average in Fig.

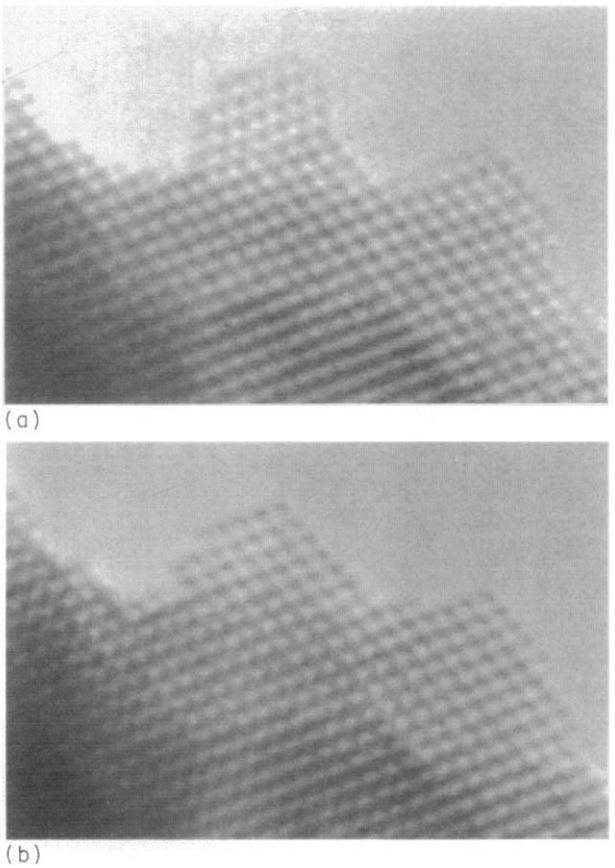

Fig. 14. (a), (b) Four-frame averages of the promontory before and after accretion to the main body of the crystal.

15 [20]. This image consists of three zones; the TbO_x substrate, a region that shows a disordered intermediate stage of decomposition, and the undecomposed hydroxide. The progress of the reaction is outwards from the substrate interface rather than, for example, nucleation on the surface and growth inwards. Figure 16(a)–(d) shows the progress of the reaction taken from the continuous video record. Figure 17 is a cartoon illustrating the mechanism of the decomposition and accretion.

7. Beam-induced reduction of PrO_2 to $Pr_{12}O_{22}$

Phase relationships in the $PrO_{2.00}$–$PrO_{1.83}$ region show a two-phase gap above 450 °C as can be seen in the phase diagram shown in Fig. 3. However, powder X-ray diffraction patterns [21] and HREM images [22] have indicated a $Pr_{16}O_{30}$ phase, ($PrO_{1.88}$), probably metastable, exists in this region. At higher temperatures, a disordered fluorite, α-phase exists.

7.1. Reduction involves a displacive structural change

PrO_2 crystallizes in the cubic, fluorite structure. Metal atoms occupy the fcc positions and oxygen atoms occupy

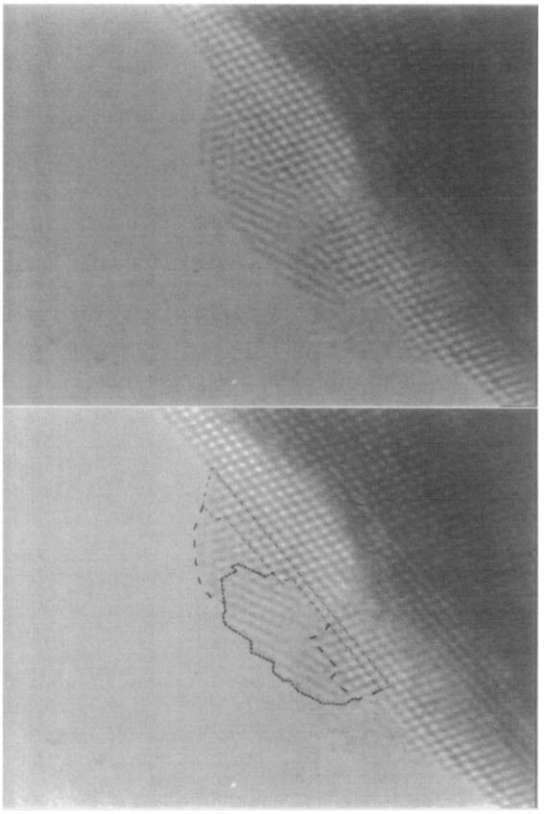

Fig. 15. An enclave of $Tb(OH)_3$ formed during leaching of $Tb_{11}O_{20}$ After Kang and Eyring [20]. The three zones are outlined.

all and only the tetrahedral interstices. The metal atoms have a cubic coordination with oxygen; the oxygen atoms are tetrahedrally coordinated by metal atoms.

$Pr_{12}O_{22}$ (β) has a monoclinic structure that is fluorite-related. Figure 8 shows the projection of the β-phase on the fluorite substructure. The composition change results from having one-twelfth of the oxygen sites vacated in an ordered way.

7.2. In situ HREM studies

The first HREM images, although primarily fluorite, already indicate loss of oxygen by the appearance of modulation streaks as clearly shown in Fig. 18. This is a four-frame averaged image with a filtered image insert [23].

The modulation becomes more regular with time and, although never perfect, corresponds to the known, metastable π-phase ($n = 16$) [22] as shown by the collage containing the image, the diffraction pattern, and the filtered image in Fig. 19.

As beam-induced reduction continues, a new modulation with a different spacing emerges and becomes quite regular even developing a superstructure (Fig. 20). The diffraction pattern shows that the new mod-

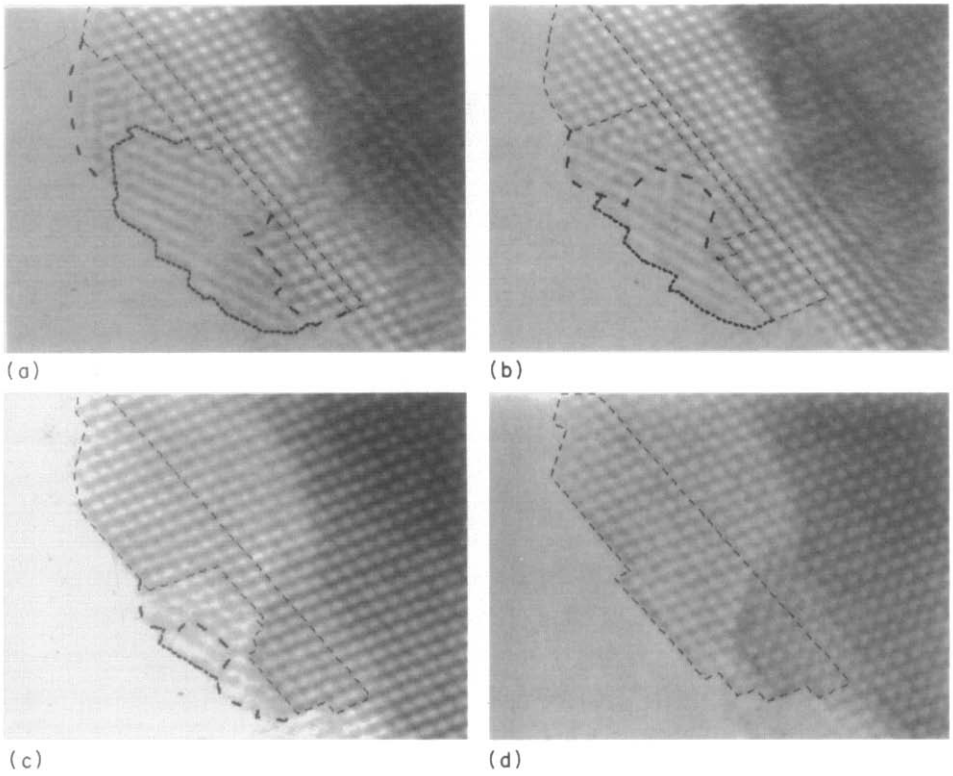

Fig. 16. (a)–(d) A sequence of four-frame images taken during the accretion of oxide formed from hydroxide decomposition on a TbO_x surface. The three zones are outlined in each image.

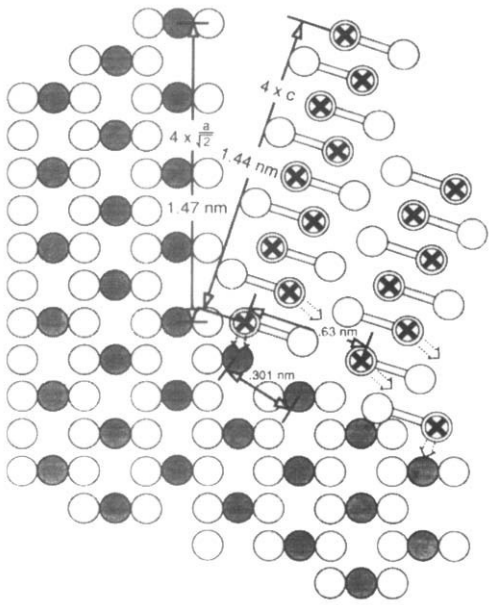

Fig. 17. The proposed juxtaposition of the structures of $Tb(OH)_3$ and TbO_x during hydroxide decomposition and accretion on the surface of TbO_x. After Kang and Eyring [20].

ulation is the precursor of the [−1 0 1] zone of the $\beta(1)$-phase. Later, another modulation developed superimposed on the old. It gradually replaced the old pattern completely. The derived diffraction pattern shows a different orientational variant of the $\beta(1)$ phase. The collage derived from a four-frame average shows the new orientational variant of the $\beta(1)$ phase, [3 2 3] (Fig. 21).

Strong beam heating causes dramatic changes in the structural development and produces still another orientational variant of $\beta(1)$, [0 1 0]. The change is especially noticeable in the surface which reconstructs according to the new structure, with appreciable transport of material. Figure 22 shows the extensive reconstruction and the relationship of the reconstructed surface to the crystallized $\beta(1)$-phase. These results are consistent with the demonstrated mobility of oxygen atoms in the fluorite-related structures and suggests much more mobile metal atoms in the surface than one would otherwise expect.

The development of modulation occurs during ordinary HREM observation. From past experience, we estimate the temperature in this experiment to be in the neighborhood of 300 °C, well below the consolute temperature. The development of the modulated structure in the region previously interpreted as consisting of a two-phase region was quite surprising and, at first glance, contrary to the X-ray powder diffraction results [6,24] which showed two phases, F and β. Perhaps, since reflections from the fluorite substructure are very strong, and the lattice parameters differ by only 2%

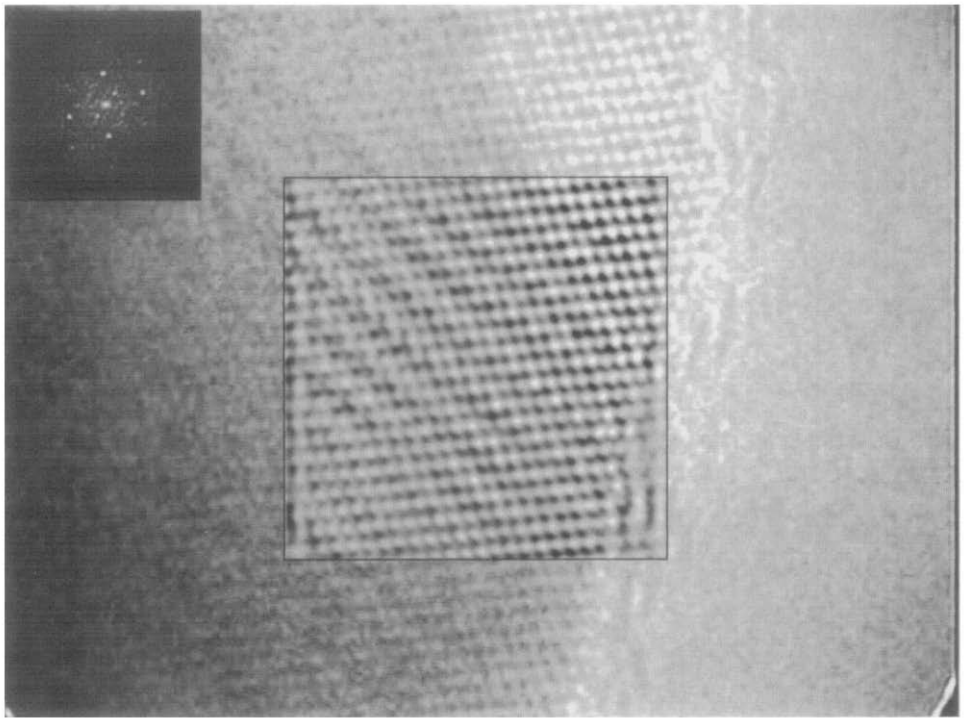

Fig. 18. Early stages in the *in situ* decomposition of PrO_2 to $Pr_{16}O_{30}$ in the HREM. After Kang and Eyring [20].

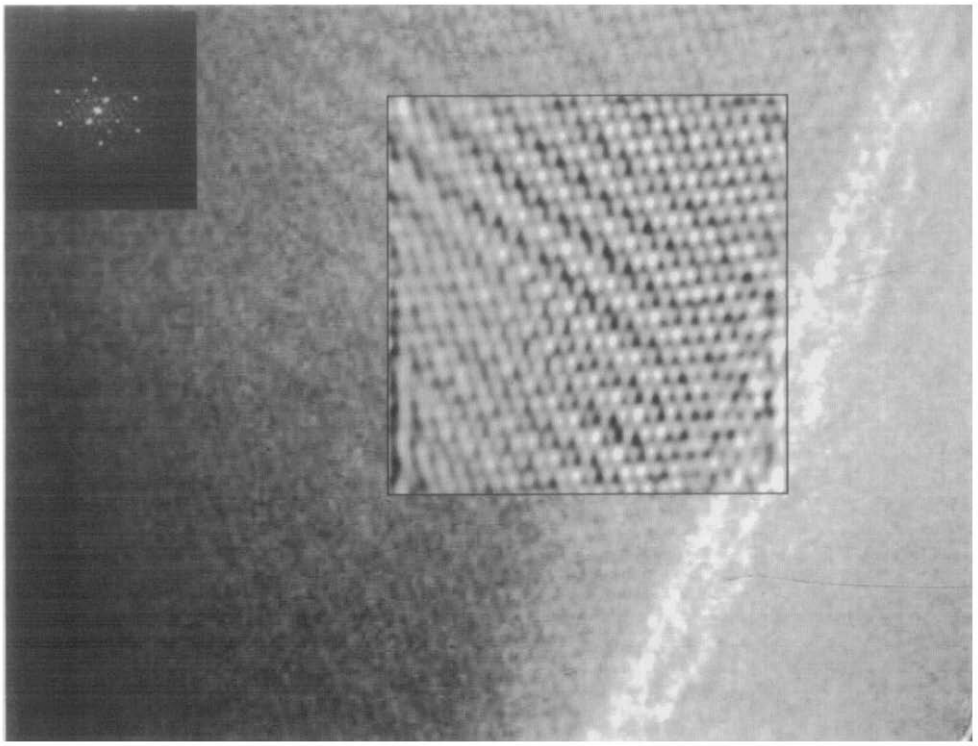

Fig. 19. The modulated structure of $Pr_{16}O_{30}$ showing the diffraction pattern and filtered image.

they might not be resolved in the electron diffraction patterns but would be in the more precise X-ray powder diffraction patterns. The modulation and superstructure spots that occur as oxygen is lost would not be apparent in the X-ray patterns, but are clear in the calculated electron diffraction patterns.

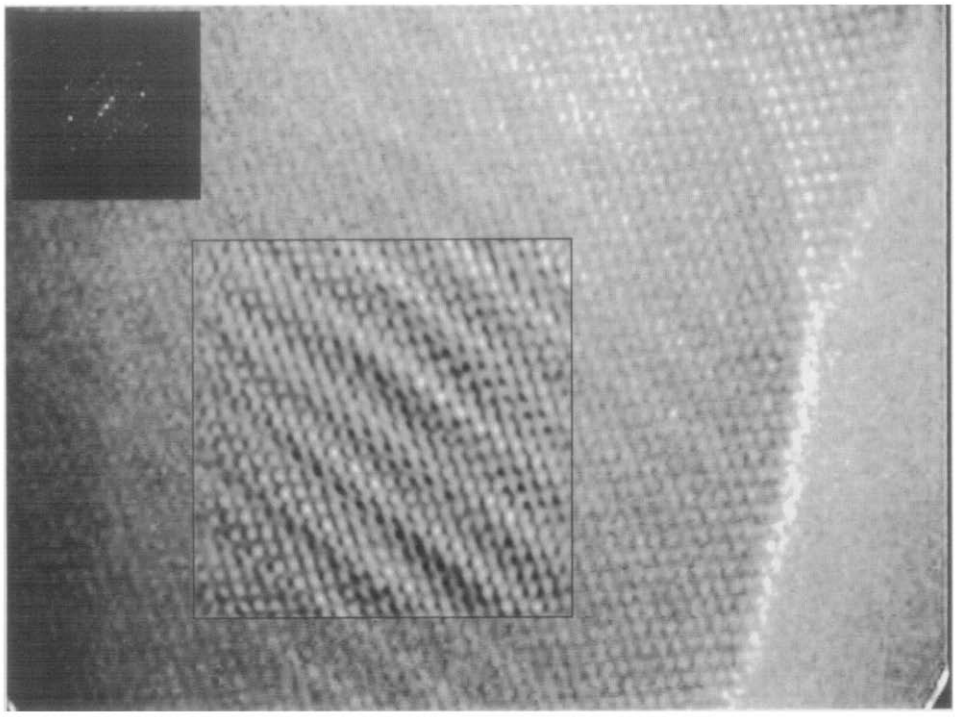

Fig. 20. The transformed modulation to the pre-beta, $Pr_{12}O_{22}$ structure in the $[-1\,0\,1]_F$ zone.

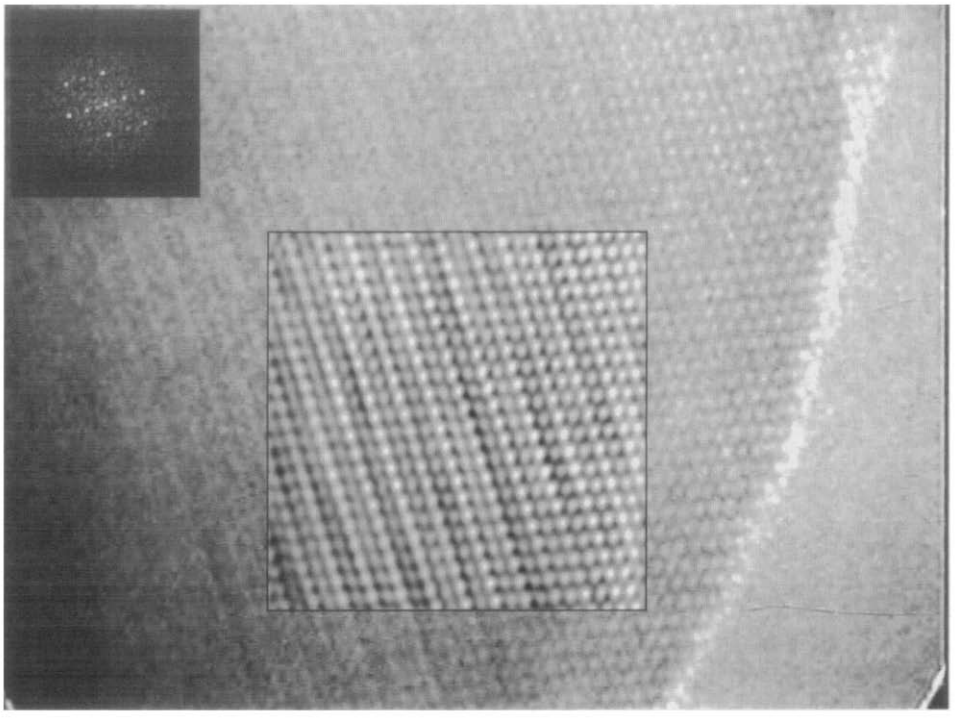

Fig. 21. An orientational transformation of the $[-1\,0\,1]_F$ zone to the $[3\,2\,3]_F$ zone in the pre-beta structure.

8. Conclusions

We have outlined the main lines of our work in characterizing the black oxide of praseodymium. We have shown the system to exhibit many esoteric behaviors of the chemical solid state. Among these are truly non-stoichiometric phases of wide composition ranges, homologous series of ordered intermediate phases that are structurally anion-deficient and fluorite-related, hysteresis in the two-phase regions. We have demonstrated the detailed if somewhat qualitative results of an HREM study of the disproportionation of a crystal of $Tb_{11}O_{20}$

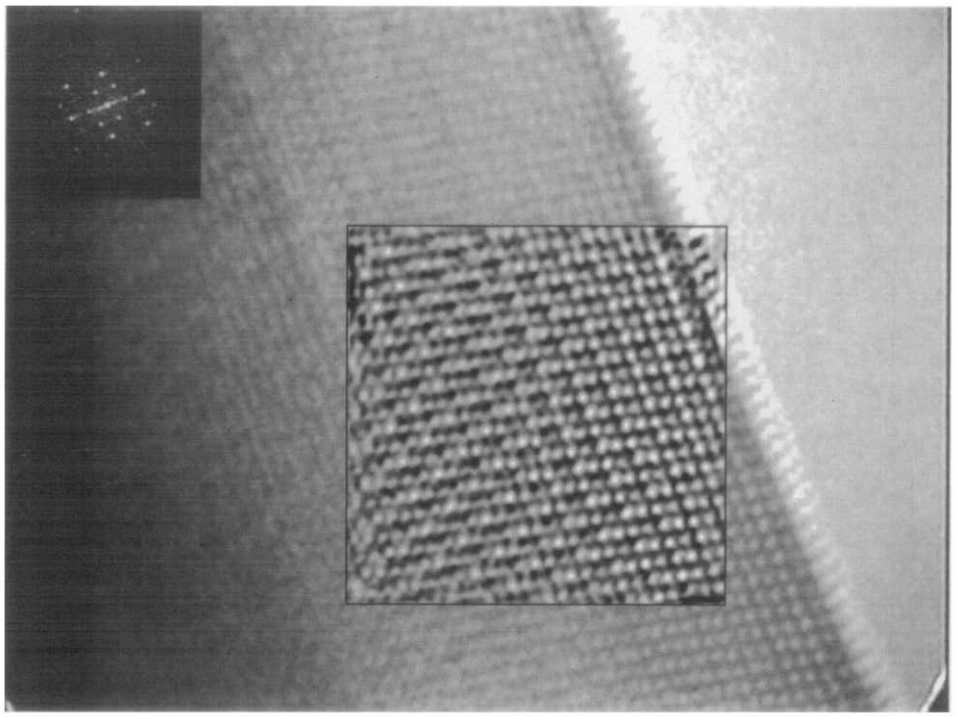

Fig. 22. A further transformation to the $[0\,1\,0]_F$ zone and the surface reconstruction during intense electron beam irradiation.

caused by contact with dilute acid that revealed the mechanism of the leaching reaction, the mechanism of removal of a twin boundary in the resulting TbO_2, and the decomposition of the $Tb(OH)_3$ formed in the surface leaching reaction.

Further, the HREM makes possible the observation of the progressive loss of oxygen from PrO_2 to $Pr_{12}O_{22}$ in what is supposed to be a two-phase region. The mechanism of this *in situ* electron-beam reduction is through modulated intermediate states that evolve into an intermediate compound as well as successive orientational variants of $Pr_{12}O_{22}$.

Acknowledgment

How does one who has, over a lifetime, depended so heavily on others, say 'thank you'? Help has come to me from students and other colleagues who have taught me, from staff who have served me, from my family who have sustained me, and from the organizations at home and abroad who have paid the bills. Without this palpable assistance, the things that have brought me here tonight could not have been done. I would like to salute this host of benefactors through a current co-worker, Zhenchuan Kang, a symbol of the colleagues who have instructed me; my secretary for 12 years, Jeanette Nickels, as a representative of faithful assistants; LaReal Eyring, my wife of more than 50 years, who epitomizes the certain source of my strength; and the acronyms, NSF and ASU, that represent the indispensible institutional support.

References

1 C. Auer von Welsbach, *Monatsh. Chem., 6* (1885) 477.
2 W. Prandtl and K. Huttner, *Z. Anorg. Allg. Chem., 149* (1925) 235.
3 W. Prandtl and G. Rieder, *Z. Anorg. Allg. Chem., 238* (1938) 225.
4 H.A. Pagel and H.M.-P. Brinton, *J. Am. Chem. Soc., 51* (1929).
5 J.K. Marsh, *J. Chem. Soc.,* (1946) 15.
6 J.D. McCullough, *J. Am. Chem Soc., 72* (1950) 1386.
7 R.E. Ferguson, E.D. Guth and L. Eyring, *J. Am. Chem. Soc., 76* (1954) 3890.
8 B.G. Hyde, D.J.M. Bevan and L. Eyring, *Philos. Trans. R. Soc. London, Ser. A, 259* (1966) 583.
9 R. Turcotte, J. Warmkessel, R.J.D. Tilley and L. Eyring, *J. Solid State Chem., 3* (1971) 265.
10 J.O. Sawyer, B.G. Hyde and L. Eyring, *Bull. Soc. Chim. Fr.,* (1965) 1190.
11 P. Kunzmann and L. Eyring, *J. Solid State Chem., 14* (1975) 229.
12 A.J. Skarnulis, E. Summerville and L. Eyring, *J. Solid State Chem., 23* (1978) 59.
13 R.T. Tuenge and L. Eyring, *J. Solid State Chem., 29* (1979) 165.
14 N.C. Baenziger, H.A. Eick, H.S. Schuldt and L. Eyring, *J. Am. Chem. Soc., 83* (1961) 2219.
15 R.B. Von Dreele, L. Eyring, A.L. Bowman and J.L. Yarnell, *Acta Crystallogr., Sect. B, 31* (1975) 971.

16 E. Schweda, D.J.M. Bevan and L. Eyring, *J. Solid State Chem., 90* (1991) 109.
17 J. Zhang, Z.C. Kang and L. Eyring, *J. Alloys Comp., 192* (1993) 57.
18 Z.C. Kang and L. Eyring, *J. Solid State Chem., 75* (1988) 60.
19 Z.C. Kang, D.J. Smith and L. Eyring, *Ultramicroscopy, 22* (1987) 71.
20 Z.C. Kang and L. Eyring, *Metal. Trans., 22A* (1991) 1223.
21 K. Otsuka, M. Kunitomi and T. Saito, *Inorg. Chim. Acta, 115* (1986) L31.
22 Z.C. Kang, J. Zhang and L. Eyring, *Aust. J. Chem., 45* (1992) 1499.
23 L. Eyring and Z.C. Kang, *Eur. J. Solid State Inorg. Chem., 28* (1991) 459.
24 C.L. Sieglaff and L. Eyring, *J. Am. Chem. Soc., 79* (1957) 3024.
25 J. Kordis and L. Eyring, *J. Phys. Chem., 72* (1968) 2044.